Pressure effects on the transition temperature and the magnetic field penetration depth in the pyrochlore superconductor $RbOs_2O_6$

R. Khasanov,[1,2,3] D.G. Eshchenko,[3,4] J. Karpinski,[5] S.M. Kazakov,[5]

N.D. Zhigadlo,[5] R. Brütsch,[6] D. Gavillet,[6] and H. Keller[3]

[1] Laboratory for Neutron Scattering,

ETH Zürich and Paul Scherrer Institut, CH-5232 Villigen PSI, Switzerland

[2]DPMC, Université de Genève, 24 Quai Ernest-Ansermet, 1211 Genève 4, Switzerland

[3]Physik-Institut der Universität Zürich,

Winterthurerstrasse 190, CH-8057, Zürich, Switzerland

[4]Laboratory for Muon Spin Spectroscopy,

PSI, CH-5232 Villigen PSI, Switzerland

[5]Solid State Physics Laboratory, ETH 8093 Zürich, Switzerland

[6]Laboratory for Material Behaviour,

Paul Scherrer Institut, CH-5232 Villigen PSI, Switzerland

Abstract

We report magnetization measurements under high hydrostatic pressure in the newly discovered pyrochlore superconductor $RbOs_2O_6$ ($T_c \simeq 6.3$ K at $p = 0$). A pronounced and *positive* pressure effect (PE) on T_c with $dT_c/dp = 0.090(1)$ K/kbar was observed, whereas no PE on the magnetic penetration depth λ was detected. The relative pressure shift of T_c [$d\ln T_c/dp \simeq 1.5$ %/kbar] is comparable with the highest values obtained for highly underdoped high-temperature cuprate superconductors. Our results suggest that $RbOs_2O_6$ is an adiabatic BCS–type superconductor.

PACS numbers: 74.70.Dd, 74.62.Fj, 74.25.Ha, 83.80.Fg

arXiv:cond-mat/0404542v1 [cond-mat.supr-con] 22 Apr 2004

There is an increasing interest to the physics of geometrically frustrated systems. One of the most remarkable examples is the observation of bulk superconductivity in pyrochlore oxide KOs_2O_6 with the transition temperature $T_c \simeq 9.6$ K [1]. It was the second compound with pyrochlore structure, after $CdRe_2O_7$ ($T_c \simeq 1$ K) [2, 3], where superconductivity was observed. Recently, the third and the forth pyrochlore superconductors, namely $RbOs_2O_6$ ($T_c \simeq 6.3$ K) [4, 5, 6, 7] and $CsOs_2O_6$ ($T_c \simeq 3.3$ K) [8] were announced. The nature of the pairing mechanism in these pyrochlore compounds is still an open question. $CdRe_2O_7$ is suggested to be a weak–coupling BCS superconductor [9] without nodes in the superconducting gap [9, 10]. Specific heat measurements performed on $RbOs_2O_6$ [5] are consistent with BCS type of behaviour. On the other hand, Hiroi *et al.* [4] and Koda *et al.* [11] pointed to an unconventional mechanism of superconductivity in KOs_2O_6 and suggested that the superconducting order parameter is anisotropic [11].

Magnetic field penetration depth λ and high-pressure studies traditionally play an important role in superconductivity. The temperature dependence of λ reflects the quasiparticle density of states available for thermal excitations and therefore probes the superconducting gap structure. In addition, the shape of $\lambda(T)$ can provide relevant information about the superconducting mechanism. High–pressure experiments, if a high pressure effect on T_c is observed, are a good indication that higher values of T_c in similar compounds may be obtained by "chemical" pressure (by changing the appropriate ion to its chemical equivalent with different ion size).

In this letter we report studies of the hydrostatic pressure effect on the superconducting temperature T_c and the magnetic field penetration depth λ in the pyrochlore superconductor $RbOs_2O_6$. The value of λ extrapolated to zero temperature is estimated to be in the range 410 nm to 520 nm. The behavior of $\lambda(T)$ indicates that $RbOs_2O_6$ is most probably a s–wave weak–coupled BCS superconductor within the adiabatic limit. However, d–wave type of pairing symmetry is not completely excluded. The transition temperature increases with increasing pressure with the slope $dT_c/dp = 0.090(1)$ K/kbar. This effect can be explained by a substantial increase of the electron-phonon coupling constant λ_{el-ph} with pressure.

Details of the sample preparation for $RbOs_2O_6$ can be found elsewhere [5, 6]. In the current work, we performed DC–magnetization measurements. In this technique, the critical temperature is directly obtained from the magnetization curve. Following the classical work

of Shoenberg [12], for fine powders with known grain sizes the magnetic penetration depth can be calculated from the Meissner fraction. For this reason the $RbOs_2O_6$ powder sample was ground. The grain size distribution was then determined by analyzing SEM (scanning electron microscope) photographs. The measured particle radius distribution $N(R)$ and the distribution of the volume fraction $\sim N(R)R^3$ are shown in Fig. 1.
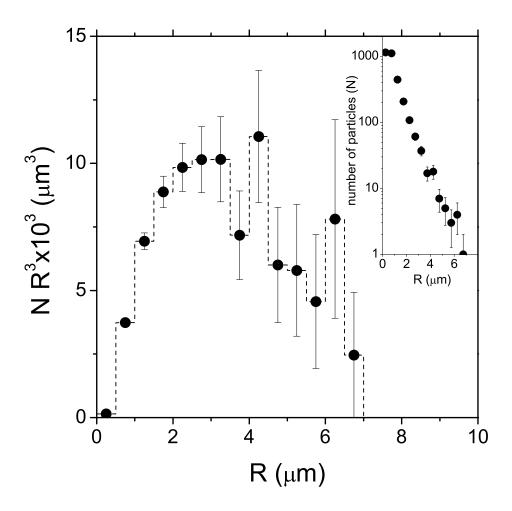

FIG. 1: The volume fraction distribution $N(R)R^3$ in the $RbOs_2O_6$ powder determined from the SEM photographs. The dashed line is the stepwise $g(R)$ function used for $\lambda(T)$ determination by means of Eq. (1). Inset shows the grain size distribution $N(R)$ in a semilogarithmic scale. Errors are statistical.

The hydrostatic pressure was generated in a copper-beryllium piston cylinder clamp espe-

cially designed for magnetization measurements under pressure [13]. The sample was mixed with Fluorient FC77 (pressure transmitting medium) with a sample to liquid volume ratio of approximately 1/6. With this cell hydrostatic pressures up to 12 kbar can be achieved [13]. The pressure was taken from a separate calibration set of magnetization experiments where a small piece of In $[T_c(0) = 3.4$ K$]$ with known $T_c(p)$ dependence was added to the sample and both T_c of In and $RbOs_2O_6$ were recorded.

The field-cooled (FC) magnetization measurements were performed with a SQUID magnetometer in a field of 0.5 mT at temperatures ranging from 1.75 K to 10 K. The absence of weak links between grains was confirmed by the linear magnetic field dependence of the FC magnetization, measured at 0.25 mT, 0.5 mT and 1.0 mT for each pressure at $T = 1.75$ K. The Meissner fraction f was calculated from the mass of the samples, their x-ray density, and assuming spherical grains. The volume of the superconducting fraction was taken 77 % in accordance with the heat capacity measurements performed with this sample [5].

The temperature dependence of the penetration depth λ was calculated from the measured $f(T)$ by using the Shoenberg formula [12] modified for the known grain size distribution [14]:

$$f(T) = \int_0^\infty \left(1 - \frac{3\lambda(T)}{R} \coth \frac{R}{\lambda(T)} + \frac{3\lambda^2(T)}{R^2}\right) g(R)\mathrm{d}R / \int_0^\infty g(R)\mathrm{d}R \quad . \tag{1}$$

Here $g(R) = N(R)R^3$, and $N(R)$ is the grain size distribution (see Fig. 1). By solving this nonlinear equation, λ for each value of f was extracted, and then the set of $\lambda(T, p)$ dependences was reconstructed. The resulting temperature dependence $\lambda^{-2}(T, 0)$ at ambient pressure is shown in Fig. 2. Reconstructed data were fitted with different models. The dotted line represents the fit with the two–fluid model $\lambda^{-2}(T)/\lambda^{-2}(0) = 1 - (T/T_c)^4$ ($T_c = 5.91(2)$ K, $\lambda(0) = 520(5)$ nm) which corresponds to a strong coupled BCS superconductor. In this paragraph, the errors in parameters are transfered from the "noise" of magnetization measurements and do not include systematic errors which are discussed later. The solid line is the fit ($T_c = 6.16(1)$ K, $\lambda(0) = 490(1)$ nm) with the tabulated Mülhschlegel data [15] calculated for a weak coupled s-wave BCS superconductor. It is seen that the weak coupling BCS behavior describes the experimental data rather well, below 5.9 K the deviation of the experimental points from the theoretical BCS curve does not exceed 2%. For comparison

4

with literature, we also performed a fit with the empirical power law $\lambda^{-2}(T)/\lambda^{-2}(0) = 1 - (T/T_c)^n$ [16] with free n (dashed line in Fig. 2). The fit yields $T_c = 6.17(1)$, $\lambda(0) = 456(3)$ nm, and $n = 1.80(3)$. In [11] an observation of $n \simeq 2$ was taken as an argument in favor of d–wave type of pairing. To distinguish between weak coupling BCS and d–wave models one has to know $\lambda^{-2}(T)$ *at low temperatures* where they exhibit completely different behavior. Unfortunately, these data are not available yet. That is why, from the current experimental data, we can not exclude completely the possibility of $d_{x^2-y^2}$ type of pairing in $RbOs_2O_6$. We plan to perform low temperature measurements in the nearest future.

To estimate the error in the *absolute* value of $\lambda(0)$ introduced by the uncertainty in the grain–size distribution we performed reconstructions with two "extreme" conditions. For the first we took the grain–size distribution in the form $N^-(R) = N(R) - \sqrt{N(R)}$, for the second we took $N^+(R) = N(R) + \sqrt{N(R)}$. Appropriate $\lambda^{-2}(T)$ dependences for $N^+(R)$, $N(R)$ and $N^-(R)$ are shown in the insert of Fig. 2. The fit with the weak–coupling BCS model yields 440(1) nm for the lowest and 520(1) nm for the highest values of $\lambda(0)$. Bearing in mind the absence of the experimental data at low temperatures and, as a result, the model dependent (power law vs weak–coupling) error in $\lambda(0)$ extrapolation procedure (which introduces additional uncertainty of about 30 nm) we can estimate the interval for $\lambda(0)$ ranging from 410 nm to 520 nm. To diminish this uncertainty more direct measurements (e.g. μSR) are planed.

As a next step we performed pressure effect (PE) measurements on T_c and λ. As it was already mentioned, the procedure of the $\lambda^{-2}(T)$ reconstruction is sensitive to the grain–size distribution. In addition it is also very sensitive to the value of the superconducting fraction, which was fixed from heat capacity measurements. The good thing here is that we study *relative* effects measured with the same sample in the same pressure cell, where most of the systematic errors are eliminated. The main systematic error for such measurements comes from misalignments of the experimental setup after the cell was removed from the SQUID magnetometer and put back again. We checked this procedure with a set of measurements at constant pressure. The systematic scattering of the magnetization data is of about 0.5%, giving a relative error in $\lambda^{-2}(T)$ of about 2%.

Figure 3 shows the λ^{-2} vs T dependences for $p = 0.0$ kbar and 9.98 kbar. The transition temperature increases almost by 1 K at 9.98 kbar, whereas there is practically no change
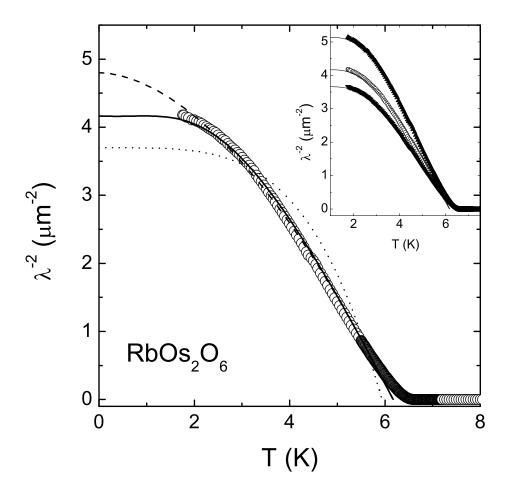
FIG. 2: The temperature dependence of λ_{ab}^{-2} for $RbOs_2O_6$ calculated from the measured $f(T)$ by using Eq. (1). Lines represent fit with the weak (solid line), strong (dotted line) coupling BCS models, and with a power law (dashed line). See text for an explanation. Inset shows $\lambda_{ab}^{-2}(T)$ dependences calculated for different grain–size distribution functions. From top to the bottom: $N^+(R)$, $N(R)$ and $N^-(R)$.

in $\lambda(0)$. The reconstructed curves are indistinguishable within the error bars after T/T_c scaling. This feature implies that $\lambda(0)$ is pressure independent with the absolute value of $\lambda(0)$ depending on the pairing model. To reduce the model dependent uncertainties, the normalized to ambient pressure magnetic penetration depth $\lambda^{-2}(0,p)/\lambda^{-2}(0,0)$ are plotted in Fig. 4. One can see that $\lambda^{-2}(0,p)/\lambda^{-2}(0,0)$ data are scattered and touching by error bars
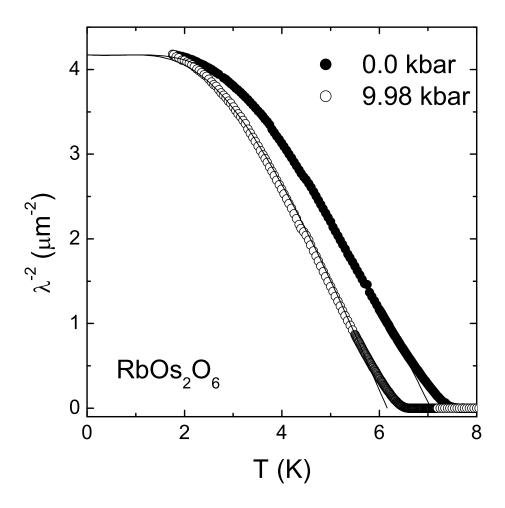
[see Fig. 4(a)].

FIG. 3: The temperature dependence of λ_{ab}^{-2} for RbOs$_2$O$_6$ obtained from $f(T)$ data at $p = 0.0$ kbar and 9.98 kbar using Eq. (1). Solid lines represent fits with the weak–coupling BCS model.

In RbOs$_2$O$_6$ an estimate of the coherence length ξ, derived from the second critical field $H_{c2}(0)$, gives $\xi \simeq 7.4$ nm [5]. Under the assumption that l has the same order of magnitude as in the pyrochlore superconductor Cd$_2$Re$_2$O$_7$ ($l \sim 20 - 70$ nm [9]), RbOs$_2$O$_6$ may be considered as a superconductor in the clean limit $l \gg \xi$. In this case λ obeys the relation:

$$\lambda \propto n_s / m^* , \tag{2}$$

where n_s is the superconducting charge carrier density, and m^* is the effective mass of the supercarriers. Therefore, the absence of a PE on $\lambda(0)$ suggests that either both quantities

n_s and m^* are pressure independent or the pressure shifts of n_s and m^* cancel each other. While we cannot rule out completely the second scenario, we think that the the first one is more likely. The conventional phonon-mediated theory of superconductivity is based on the Migdal adiabatic approximation in which the effective supercarrier mass m^* is independent of the lattice degrees of freedom. Thus, the absence of a PE on $\lambda(0)$ [see Fig 4(a)] suggests that $RbOs_2O_6$ may be considered as an adiabatic BCS superconductor. Note that the same effect (absence of a PE on λ) was observed recently in MgB_2 which is accepted to be a purely phonon mediated superconductor [17].

The pressure dependence of the critical temperature is shown in Fig. 4(b). The linear fit yields $dT_c/dp = 0.090(1)$ K/kbar. The linear increase of T_c with pressure observed in $RbOs_2O_6$ is quite unusual. For the majority of BCS–type superconductors (including MgB_2) T_c decreases with increasing pressure. For conventional superconductors the pressure shift of T_c can be derived as [18, 19]

$$\frac{d \ln T_c}{dp} = \frac{d \ln \langle \omega \rangle}{dp} + \frac{1.23 \lambda_{el-ph}}{(\lambda_{el-ph} - 0.11)^2} \frac{d \ln \lambda_{el-ph}}{dp} \ , \tag{3}$$

where $\langle \omega \rangle$ is the average phonon frequency, and λ_{el-ph} is the electron–phonon coupling constant. There are two contributions to the pressure shift of T_c: from the phonon system $[d \ln \langle \omega \rangle / dp]$ and from the coupling between electron and phonon subsystems $[d \ln \lambda_{el-ph}/dp]$. The effect of pressure on the phonon spectra usually results in an increase of the average phonon frequency, and the first term in Eq. (3) is generally positive. An estimate of a typical range of $d\langle \omega \rangle / dp = -\gamma/B$ (where $\gamma = d \ln \langle \omega \rangle / d \ln V$ is the Grüneisen parameter, V is the volume, and B is the bulk modulus) in conventional superconductors gives $d\langle \omega \rangle / dp \approx 0.01\% - 0.5\%$ per kbar [20, 21]. The pressure shift of T_c found in our study ($d \ln T_c/dp \simeq 1.5\%$/kbar) is much bigger than the possible contribution form the first term in Eq. (3). Therefore, our results suggest a substantial increase of λ_{el-ph} with pressure. Alternatively, the positive pressure effect on T_c can be explained by a sort of charge ordering, resulting in the disproportionation of the Os tetrahedra [22].

In conclusion, we performed magnetization measurements in the newly discovered superconductor $RbOs_2O_6$ under hydrostatic pressure. The absolute value of λ at zero temperature and ambient pressure is estimated to be in the range 410–520 nm. The temperature dependence of the magnetic penetration depth λ is consistent with that expected for a weak–coupled s–wave BCS superconductor. However, to rule out completely d–wave symmetry,

additional low temperatures measurements are required. A pronounced and *positive* pressure effect on T_c with $\mathrm{d}T_c/\mathrm{d}p = 0.090(1)$ K/kbar was observed, in contrast to the negative pressure shift generally detected in conventional superconductors. This finding can be explained within the framework of BCS theory under the assumption that the electron-phonon coupling constant λ_{el-ph} increases with pressure. The absence (within the experimental uncertainties) of the pressure effect on λ suggests that $RbOs_2O_6$ is an adiabatic BCS–type superconductor.

[1] S. Yonezawa, Y. Muraoka, Y. Matsushita, and Z. Hiroi, J.Phys.: Cond.Mat. **16**, L9 (2004).

[2] M. Hanawa, Y. Muraoka, T. Tayama, T. Sakakibara, J. Yamaura, and Z. Hiroi, Phys. Rev. Lett. **87**, 187001 (2001).

[3] H. Sakai, K. Yoshimura, H. Ohno, H. Kato, S. Kambe, R.E. Walstedt, T.D. Matsuda, Y. Haga, and Y. Onuki, J.Phys.: Cond.Mat. **13**, L785 (2001).

[4] Z. Hiroi, S. Yonezawa, and Y. Muraoka, arXiv:cond-mat/0402006.

[5] M. Brühwiler, S.M. Kazakov, N.D. Zhigadlo, J. Karpinski, and B. Batlogg, arXiv:cond-mat/0403526.

[6] S.M. Kazakov, N.D. Zhigadlo, M. Brühwiler, B. Batlogg, and J. Karpinski, arXiv:cond-matt/0403588.

[7] S. Yonezawa, Y. Muraoka, Y. Matsushita, and Z. Hiroi, J. Phys. Soc. Jpn **73**, 819 (2004).

[8] S. Yonezawa, Y. Muraoka, and Z. Hiroi, arXiv:cond-mat/0404220.

[9] Z. Hiroi and M. Hanawa, J. Phys. Chem. Solids **63**, 1021 (2002).

[10] M.D. Lumsden, S.R. Dunsiger, J.E. Sonier, R.I. Miller, R.F. Kiefl, R. Jin, J. He, D. Mandrus, S.T. Bramwell, and J.S. Gardner, Phys. Rev. Lett. **89**, 147002 (2001).

[11] A. Koda, W. Higemoto, K. Ohishi, S.R. Saha, R. Kadono, S. Yonezawa, Y. Muraoka, and Z. Hiroi, arXiv:cond-matt/0402400.

[12] D. Shoenberg, Proc. R. Soc. Lond. **A 175**, 49 (1940).

[13] T. Straessle, Ph.D thesis, ETH Zurich, 2001.

[14] A. Porch, J.R. Cooper, D.N. Zheng, J.R. Waldram, A.M. Campbell, and P.A. Freeman, Phycica C **214**, 350 (1993).

[15] B. Mühlschlegel, Z. Phys. **155**, 313 (1959).

[16] P. Zimmermann, H. Keller, S. L. Lee, I. M. Savic, M. Warden, D. Zech, R. Cubitt, E. M. Forgan, E. Kaldis, J. Karpinski, and C. Krüger, Phys. Rev. B **52**, 541 (1995).

[17] D. Di Castro *et al.*, unpublished.

[18] W.L. McMillan, Phys. Rev. **167**, 331 (1968).

[19] R.E. Hodder, Phys. Rev. **180**, 530 (1969).

[20] P.E. Seiden, Phys. Rev. **179**, 458 (1969).

[21] *www.webelements.com.*

[22] Z. Hiroi, T. Yamauchi, T. Yamada, M. Hanawa, Y. Ohishi, O. Shimomura, M. Abliz, M. Hedo, and Y. Uwatoko, J. Phys. Soc. Jpn. **71**, 1553 (2002).
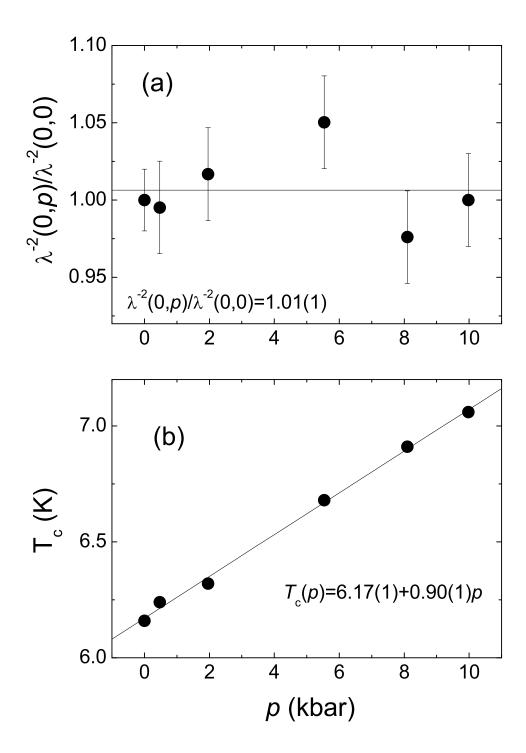
FIG. 4: The pressure dependence of $\lambda^{-2}(0)(p)/\lambda^{-2}(0)(p=0)$ (a) and T_c (b) in $RbOs_2O_6$. The solid lines are fits with parameters shown in the figure.